European Commission | Funding & tender opportunities
Single Electronic Data Interchange Area (SEDIA)

H2020-MSCA-IF-2020

Secure Indoor Communication empowered by Intelligent reflecting Surface (SICIS)

D1.2

Report on indoor MIMO channel models incorporating IRS

Authors(s)	Sai Xu, Zeyang Li, Jie Zhang
Author(s) Affiliation	University of Sheffield, UK
Editor(s):	Sai Xu
Status-Version:	V1.0
Project Number:	101032170
Project Title:	Secure Indoor Communication empowered by Intelligent reflecting Surface
Project Acronym:	SICIS
Work Package Number	2

Abstract

Both reconfigurable intelligent surfaces (RISs) and ultra-dense (UD) small-cell (SC) base stations (BSs) are investigated for indoor mmWave wireless coverage enhancement. To explore which deployment strategy is more cost-effective, the costs of deploying both RISs and UD SCs are defined and calculated. Through jointly analyzing coverage probability and network cost in typical indoor environments, we conclude that the same network coverage can be achieved by multiple deployment strategies. To achieve certain level of coverage probability with the lowest network cost, a proper number of BSs are crucial for RIS-assisted networks.

The results presented in this deliverable have addressed the requirement of Task 1.2 in the SICIS project.

Keywords: Reconfigurable intelligent surfaces, ultra-dense small-cell, mmWave communication, indoor wireless networks, coverage enhancement.

Table of Contents

1. Introduction

It is predicted that wireless data traffic will rise by up to 1000 times in the next decade, with nearly 80% of data traffic consumed indoors [1]. Meanwhile, due to the spectral resource shortage in microwave frequencies, millimeter-wave (mmWave) frequencies have been employed on wireless communication, which suffer severe wall penetration loss in indoor environments [2], [3]. Both the rapidly growing data traffic demand and high wall penetration loss of mmWave bring great challenges to indoor mmWave network deployment. Fortunately, two promising technologies can address the problem: Ultra-dense (UD) small-cell (SC) and reconfigurable intelligent surfaces (RISs).

The basic idea of UD SC is to densely deploy small cells, i.e., fully-functioning base stations (BSs) (femtocells and picocells) and radio access points (Remote Radio Heads (RRHs)), to satisfy the immense traffic demand [4]. However, the smallcell density cannot grow infinitely due to fundamental limits of network densification [5]. The wireless coverage can be maximized by reaching certain cell density, and decrease with further increase of cell density [6], [7]. In [8], the indoor network coverage is analyzed based on Poisson grid blockage model. The indoor multi-story small-cell networks are investigated in [9]. The results in [8], [9] show that wall penetration loss has a great impact on indoor network coverage.

On the other hand, RIS is an alternative technology for indoor coverage enhancement. A RIS is a meta-surface with unit cells (integrated electronic circuits), each unit cell can implement phase shift and modify amplitude on the incident signal independently. RISs can provide additional transmission paths by altering reflected signal propagation [10]. The RIS deployment is particularly useful when the line-of-sight (LoS) transmission is blocked or not strong enough [11], [12]. This makes RIS an alternative technology for coverage enhancement. The work in [13] shows that the coverage probability of RIS-assisted wireless networks is higher compared with the networks without RISs. A closed-form expression of the outage probability for RIS-assisted networks with spatially correlated channels is derived in [14], the results show that the outage probability decreases significantly after considering the spatial correlation. In addition, achievable data rate and error performance of indoor and outdoor RIS-assisted wireless networks are investigated in [15] and shown great improvement.

Even though previous research has shown that both UD SC and RIS can enhance the network coverage, it remains unknown which technology is more efficient in terms of coverage enhancement. Moreover, whether combining both technologies will result in better coverage performance than only employing anyone of them has never been investigated.

This report compares the performance of UD SC and RIS and to make the best use of both for cost-effective indoor coverage. We first define the cost of deploying UD SC BSs and RISs. Then, we present a joint analysis of coverage probability and network cost. Our main observations are that: 1) the same coverage probability can be achieved by different network deployment strategies, i.e., fewer BSs and more RISs, more BSs and fewer RISs, and only BSs; 2) a proper number of BSs are crucial to achieve certain level of coverage probability with the lowest network cost; and 3) a minimal number of BSs are required for high network coverage even with the assistance of RISs.

2. System Model

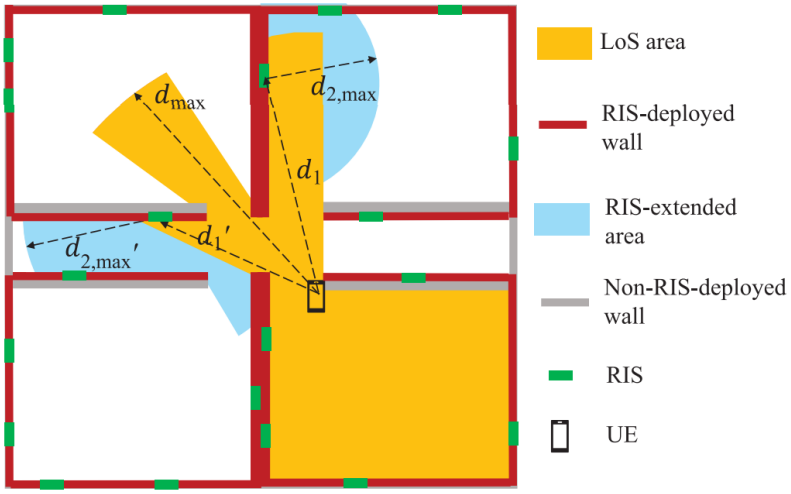

Fig. 1. The LoS area and RIS-extended area of a randomly located UE in the indoor environment.

The system model of the wireless networks in the indoor environment is presented in this section. To investigate general scenarios, both Poisson point process (PPP) [16] and Binomial point process (BPP) [17] are employed for BS distribution. The BS density is denoted by ψ_b. PPP is adopted for more general scenarios where a various number of BSs are deployed, and BPP is employed for the scenarios where a fixed number of BSs are deployed. The assumption that BS distribution follows PPP is also used in the existing works regarding indoor networks [8], [9]. The typical user equipment (UE) is randomly distributed in the indoor environment. The locations of RISs are assumed to follow one-dimensional PPP on the RIS deployed walls, as shown in Fig. 1. The RIS density is ψ_r. The length of all the RIS-deployed walls in the considered indoor layout is expressed by ξ. On the other hand, no RIS is deployed on the non-RIS-deployed walls, since no coverage gain can be obtained by deploying RISs on these walls.

Two types of transmission, i.e., the direct transmission from the BS to the UE and the RIS-assisted transmission, are considered. In addition, Rician fading channel and Rayleigh fading channel are adopted for LoS transmission and NLoS transmission, respectively. The wavelength of the signal is denoted by λ and the path loss exponent is α. Let P_t and d denote the transmit power and the transmission distance, respectively. Furthermore, the received signal power of the direct transmission from the BS to the UE is as follows:

$$P_{\mathrm{r}} = \begin{cases} \frac{P_{\mathrm{t}}|h|^2\lambda^2}{16\pi^2 d^{\alpha}}, & n_{\mathrm{w}} = 0, \\ \frac{P_{\mathrm{t}}\omega^{n_{\mathrm{w}}}|g|^2\lambda^2}{16\pi^2 d^{\alpha}}, & \text{otherwise}, \end{cases}$$

where ω denotes the wall penetration loss and n_w represents the number of passed walls. h and g follow Rician distribution and Rayleigh distribution, respectively.

The RIS-assisted transmission is adopted when the following two conditions are met: 1) the direct transmission from the BS to the UE suffers from severe wall penetration loss; 2) the transmission from the BS to the RIS and from the RIS to the UE is LoS transmission. To analyze the RIS-assisted transmission, the physical properties of the RIS must be considered. Each RIS is made of M × N unit cells, hence, the total number of unit cells per RIS is $\kappa = MN$. The size of each unit cell is $d_u \times d_u$. We assume that the power radiation pattern of RIS is independent of the incident/reflected angle of the signal and consider peak radiation in all the directions.

All the unit cells have the same amplitude value A of the reflection coefficient but different phase shift [20]. By aligning in phase of the reflected signals from the unit cells, the received signal power can be enhanced. In this report, we investigate an upper bound of the RIS-assisted network coverage by assuming perfect phase shift control. Hardware imperfections [18], [19], e.g., discrete phase shifts and phase-dependent reflection coefficient amplitude, will be analyzed in the future works. Moreover, the received signal power of the RIS-assisted transmission is formulated as [15], [20]:

$$P_{\mathrm{r}} = \frac{P_{\mathrm{t}} G \left(\sum_{i=1}^{\kappa} \phi_i \varphi_i\right)^2 d_{\mathrm{u}}^2 \lambda^2 A^2}{64\pi^3 d_1^2 d_2^2},$$

where G is the gain of the unit cell, φ_i and ϕ_i, which follow Rician distribution, represent the channel fading coefficient of the BS to the ith unit cell link and of the ith unit cell to the UE link, d_1 and d_2 denote the distance between the UE and the RIS, the distance between the BS and the RIS. We assume that walls cannot reflect signals unless RISs are deployed and signals can only be reflected one time.

3. Coverage Probability and Cost Analysis

To enhance the wireless coverage of the indoor mmWave networks, the two options are RIS deployment and SC densification. To investigate which option is more cost-effective, we define coverage probability and network cost for the RIS-assisted networks and UD SC networks.

3.1. Coverage Probability

The coverage probability is defined as the probability that the received signal power from at least one BS is higher than the power threshold T. T can be understood as the minimum received signal power that a receiver can detect. In other words, outage happens only when the signals from all the BSs are undetectable by the UE. Then, the coverage probability can be expressed as follows:

$$C = \Pr\{P_{\mathrm{r}} \geq T\}.$$

C can be calculated by Monte-Carlo simulations with η simulation times.

Algorithm 1 The Coverage Probability Calculation Algorithm

```
Generate walls according to the considered indoor layout;
for Different BS density ψ_b do
    for Different RIS density ψ_r do
        Let χ = 0;
        for i = 1 : η do
            Generate a randomly distributed UE in the considered indoor layout;
            Generate randomly distributed BSs with BS density ψ_b in the considered indoor layout;
            Generate randomly distributed RISs with RIS density ψ_r on the RIS-deployed walls;
            Calculate the received signal power from each BS using equation (1) or (2);
            if the received signal power from at least one BS satisfy P_r ≥ T then
                χ = χ + 1;
            end if
        end for
        The coverage probability C(ψ_b, ψ_r) = χ/η.
    end for
end for
```

Algorithm 1 shows Monte-Carlo simulations for the coverage probability considering fading channels and wall penetration loss. For each different BS density, η times of simulations need to be

run. In addition, the time of each simulation rises as the BS density increases. Accordingly, Algorithm 1 is very time-consuming and inconvenient for network coverage analysis. Therefore, we propose Algorithm 2 whose simulation time is not affected by the increase of BS density. In addition, the simulation results can be applied for different BS density. The principle of Algorithm 2 is presented in the following paragraphs.

According to the properties of mmWave frequency, two assumptions are made for the transmission model in Algorithm 2: 1) due to the high wall penetration loss of mmWave [2], we assume that signals cannot penetrate walls; 2) since small-scale fading is not significant in the LoS mmWave transmission [21], [22], a deterministic channel model is employed. Furthermore, given the power threshold T, the maximum LoS transmission distance is computed by:

$$d_{\max} = \frac{\lambda^{\frac{2}{\alpha}}}{(4\pi)^{\frac{2}{\alpha}} T^{\frac{1}{\alpha}}} P_{\mathrm{t}}^{\frac{1}{\alpha}}.$$

For RIS-assisted transmission, given the distance d_1 between the UE and the RIS, the maximum distance $d_{2,\max}$ between the BS and the RIS is represented as:

$$d_{2,\max} = \sqrt{\frac{GM^2N^2d_{\mathrm{u}}^2\lambda^2A^2}{64\pi^3d_1^2T}P_{\mathrm{t}}}.$$

Note that $d_{2,\max} \leq d_{\max}$.

Based on the assumptions, the LoS area and RIS-extended area of a randomly located UE in the indoor environment are shown in Fig. 1. The boundary of the LoS area is determined by either the maximum LoS transmission distance or the wall which blocks the UE. In Fig. 1, 6 RISs are located in the LoS area of the UE, but only 2 of them have the RIS-extended area which is not overlapped with the LoS area. The boundary of the RIS-extended area is decided by either the maximum reflected transmission distance or the wall which blocks the RIS. Moreover, the two scenarios that a UE is in network coverage are: 1) a BS is located in the LoS area; 2) a BS is located in the RIS-extended area. We denote the size of the LoS area and the RIS-extended area by SL and $S_\Delta(\psi_r)$, respectively. Note that $S_\Delta(\psi_r)$ is a function of RIS density ψ_r. In addition, the average number of BSs in PPP scenario and the number of BSs in BPP scenario are expressed by $nBS = \psi_b WL$. The average number of RISs is denoted by $nRIS = \psi_r \xi$.

For the scenario that the locations of BSs follow PPP, the probability that no BS is located in the LoS area and the RIS-extended area is $P_{out} = \exp(-\psi_b(S_L + S_\Delta(\psi_r)))$ [16]. Accordingly, the network coverage probability can be expressed by:

$$C_{\mathrm{PPP}} = 1 - \exp(-\psi_{\mathrm{b}}(S_{\mathrm{L}} + S_{\Delta}(\psi_{\mathrm{r}}))).$$

For the scenario that the locations of BSs follow BPP, the probability that no BS is located in the LoS area and the RIS extended area is

$$P_{\mathrm{out}} = (1 - \frac{S_{\mathrm{L}}+S_{\Delta}(\psi_{\mathrm{r}})}{WL})^{n_{\mathrm{BS}}}.$$

Therefore, the network coverage probability can be expressed by:

$$C_{\mathrm{BPP}} = 1 - \left(1 - \frac{S_{\mathrm{L}} + S_{\Delta}(\psi_{\mathrm{r}})}{WL}\right)^{n_{\mathrm{BS}}}.$$

S_L and S_Δ are obtained by Monte-Carlo simulations. Let τ be the Monte-Carlo simulation times. The procedures of the simulation are shown in Algorithm 2.

Algorithm 2 The Coverage Area Calculation Algorithm

Generate walls according to the considered indoor layout;
Divide the whole indoor area into $k \times k$ unit square with size S_{unit};
for Different RIS density ψ_{r} **do**
  for $i = 1 : \tau$ **do**
    Generate a randomly distributed UE in the considered indoor layout;
    Generate randomly distributed RISs with RIS density ψ_{r} on the RIS-deployed walls;
    Find all the RISs located in the LoS area of the UE;
    Let $S_{\text{L}} = 0$ and $S_{\Delta} = 0$;
    for $j = 1 : k^2$ **do**
      if {the distance between the UE and the center of the jth unit square does not exceed $d_{\max}$} && {no wall blocks the UE from the center of the jth unit square} **then**
        $S_{\text{L}} = S_{\text{L}} + S_{\text{unit}}$;
      else if {no wall blocks the center of the jth unit square from the RIS which locates in the LoS area} && {the distance between the RIS and the center of the jth unit square does not exceed $d_{2,\max}$} **then**
        $S_{\Delta} = S_{\Delta} + S_{\text{unit}}$;
      end if
    end for
    For different BS density ψ_{b}, calculate the coverage probability using the equation (6) and (7);
  end for
  Calculate the average coverage probability $C(\psi_{\text{b}}, \psi_{\text{r}})$.
end for

3.2. Cost Analysis

The network cost includes deployment cost and operational cost. For deployment cost, some facilities are the prerequisites for both the UD SC networks and RIS-assisted networks, e.g., both require an indoor broadband connection for providing connectivity to the BSs as backhaul. The common facilities for both networks are not considered into the cost since our aim is to compare the difference. The work in [23] defines the unit cost which is determined by the cost per equipment, the time length of the installment and the interest rate. Moreover, the total network cost is that the quantity of the network equipments multiples with the unit cost. Hence, we denote the unit cost of BSs and RISs by a_{BS} and a_{RIS}, respectively. Furthermore, the costs of BSs are that the average number of BSs multiples with the BS unit cost, i.e., $\eta_{\text{BS}} = n_{\text{BS}} a_{\text{BS}}$. And the costs of RISs are that the average number of RISs multiples with the RIS unit cost, i.e., $\eta_{\text{RIS}} = n_{\text{RIS}} a_{\text{RIS}}$. Hence, the expression of the total network cost is provided as follows:

$$\eta = \eta_{\text{BS}} + \eta_{\text{RIS}} = a_{\text{BS}} \psi_{\text{b}} WL + a_{\text{RIS}} \psi_{\text{r}} \xi.$$

The coverage probability and the network cost are correlated, since both are the functions of the BS density and the RIS density, i.e., $C(\psi_{\text{b}}, \psi_{\text{r}})$ and $\eta(\psi_{\text{b}}, \psi_{\text{r}})$. Hence, the function of the coverage probability to the network cost, i.e., $\eta(C)$, can be built. Moreover, we can find out the more costeffective network by comparing $\eta(C)$ of the UD SC networks and that of the RIS-assisted networks. Specifically, when the UD SC networks and the RIS-assisted networks have the same coverage probability, i.e., $C(\psi_{\text{b1}}, 0) = C(\psi_{\text{b2}}, \psi_{\text{r}})$, the network with lower network cost is more cost-effective than the network with higher network cost.

4. NUMERICAL RESULTS

In this section, the coverage probabilities of RIS-assisted networks and UD SC networks are evaluated, respectively. Moreover, the cost effectiveness of RIS deployment and that of UD SC deployment are compared.

The considered indoor layouts are shown in Fig. 2. The size of each room is $L_r \times L_r$. The size of the door in each room is denoted by Wd. In addition, the width of the corridor is W_c. The Rician fading parameter K = 10dB and the Rayleigh fading coefficient g ~ CN (0, 1). Antenna4 and Antenna8: The two legends denote the optimization schemes for the conventional uplink coordinated multi-cell MIMO network, in which each UE employs active antennas ('4' and '8' denote the antenna number) to communicate with BSs without the deployment of PB.

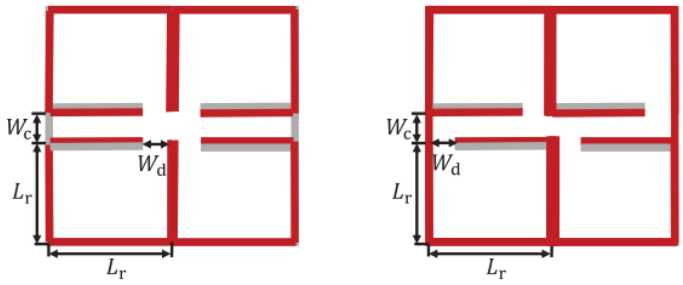

(a) Layout 1 (b) Layout 2

Fig. 2. The considered indoor layouts.

Based on Algorithm 1, the network coverage probability with different BS density and RIS density is shown in Fig. 3. The RIS with 50 × 50 unit cells is employed. Note that when RIS density is 0, only UD SC networks are employed. Fig. 3 indicates that: the coverage probability rises significantly as RIS density increases from 0 to 0.2. Further increase of RIS density can only lead to slight growth of the coverage probability. More importantly, the same coverage probability can be achieved by multiple deployment strategies, i.e., fewer BSs and more RISs, more BSs and fewer RISs, and only BSs. To find out which strategy is the most cost-effective, we need to jointly analyze the coverage probability and network cost.

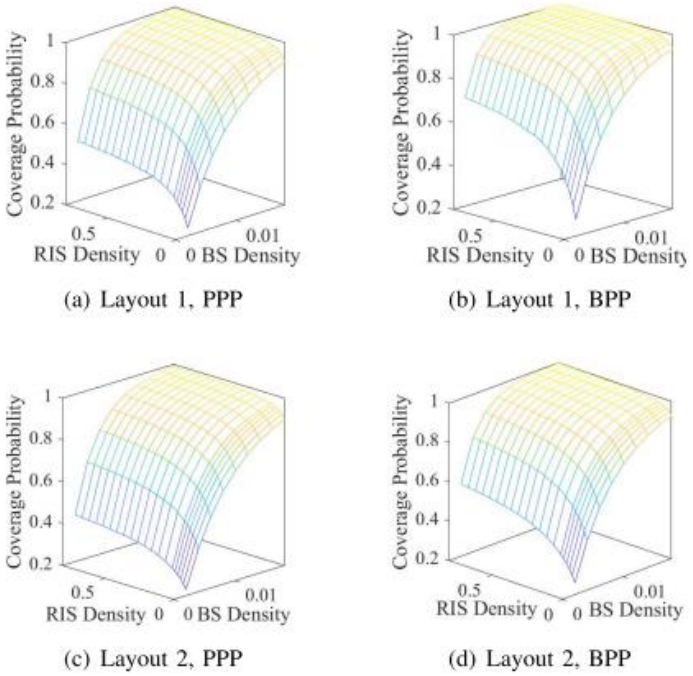

(a) Layout 1, PPP (b) Layout 1, BPP

(c) Layout 2, PPP (d) Layout 2, BPP

Fig. 3. The network coverage probability with different BS density and RIS density

In each subfigure of Fig. 4 and Fig. 5, the coverage probabilities obtained from both Algorithm 1 and Algorithm 2 are shown, and the comparison of the network cost between RIS assisted networks and UD SC networks is presented. Without loss of generality, we normalise the unit cost of UD SC BSs as 1. And

the unit cost of RISs is assumed to be 20 times lower than the unit cost of UD SC BSs. Fig. 4 and Fig. 5 can be understood as: with the same network cost, different deployment strategies can be adopted, i.e., fewer BSs and more RISs, more BSs and fewer RISs, and only BSs. Each deployment strategy leads to a different coverage probability. Note that the indoor coverage considering deterministic channels has the same trend as the indoor coverage considering fading channels and wall penetration loss, and the two indoor coverage probabilities are very close to each other. Therefore, Algorithm 2 can be adopted for performance analysis with little accuracy loss. To achieve certain level of coverage probability with the lowest network cost, a proper number of BSs are crucial, e.g., in Fig. 4(a), RISs with 4 BSs have the lowest network cost to achieve 82% coverage, compared with 7 BSs without RIS and RISs with 2 BSs. In addition, to achieve high coverage probability, i.e., above 90%, a minimal number of BSs are required, even with the assistance of RISs, e.g., 2 BSs with RISs are not cost-effective to achieve high coverage. On the other hand, the indoor layouts have a great impact on the cost-effectiveness of the RIS-assisted networks, e.g., for the scenario that the BS distribution follows BPP, in layout 1, RISs with 2 BSs have lower cost to achieve 80% coverage than BSs without RIS, while it is the exact opposite in layout 2.

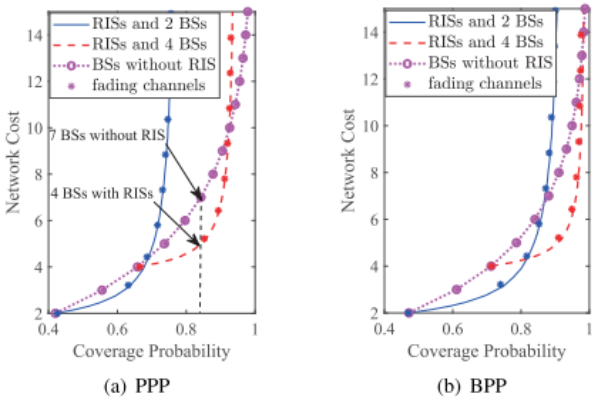

Fig. 4. The cost comparison between RIS deployment and small-cell BS densification to achieve same coverage probability in indoor layout 1.

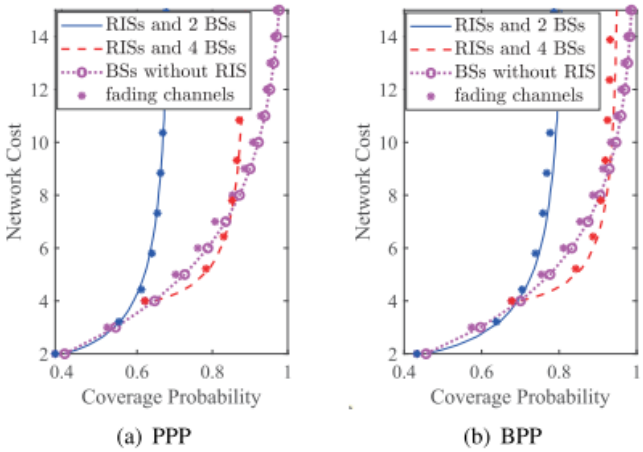

Fig. 5. The cost comparison between RIS deployment and small-cell BS densification to achieve same coverage probability in indoor layout 2.

5. Conclusion

The focus of the research presented the roles of SC densification and RIS deployment in coverage enhancement for indoor mmWave wireless networks. SC densification is essential to

achieve the adequate indoor network coverage probability. With insufficient SC BSs, no matter how densely RISs are deployed, the adequate indoor network coverage probability may not be achieved. Meanwhile, deployment of RIS is capable of notably reducing the network cost for specific circumstances while maintaining the indoor network coverage probability achieved by SC densification.

References

1. Huawei. (Feb. 2016). Five Trends to Small Cell 2020. [Online]. Available: http://www-file.huawei.com/~/media/CORPORATE/PDF/ News/Five-Trends-To-Small-Cell-2020-en.pdf
2. T. S. Rappaport et al., "Millimeter wave mobile communications for 5G cellular: It will work!" *IEEE Access*, vol. 1, pp. 335–349, 2013.
3. F. Boccardi, R. W. Heath, A. Lozano, T. L. Marzetta, and P. Popovski, "Five disruptive technology directions for 5G," *IEEE Commun. Mag.*, vol. 52, no. 2, pp. 74–80, Feb. 2014.
4. M. Kamel, W. Hamouda, and A. Youssef, "Ultra-dense networks: A survey," *IEEE Commun. Surveys Tuts.*, vol. 18, no. 4, pp. 2522–2545, 4th Quart., 2016.
5. J. G. Andrews, X. Zhang, G. D. Durgin, and A. K. Gupta, "Are we approaching the fundamental limits of wireless network densification?" *IEEE Commun. Mag.*, vol. 54, no. 10, pp. 184–190, Oct. 2016.
6. D. López-Pérez, M. Ding, H. Claussen, and A. H. Jafari, "Towards 1 Gbps/UE in cellular systems: Understanding ultra-dense small cell deployments," *IEEE Commun. Surveys Tuts.*, vol. 17, no. 4, pp. 2078–2101, 4th Quart., 2015.
7. M. Ding, P. Wang, D. López-Pérez, G. Mao, and Z. Lin, "Performance impact of LoS and NLoS transmissions in dense cellular networks," *IEEE Trans. Wireless Commun.*, vol. 15, no. 3, pp. 2365–2380, Mar. 2016.
8. J. Lee, X. Zhang, and F. Baccelli, "A 3-D spatial model for in-building wireless networks with correlated shadowing," *IEEE Trans. Wireless Commun.*, vol. 15, no. 11, pp. 7778–7793, Nov. 2016.
9. C. Chen, Y. Zhang, J. Zhang, X. Chu, and J. Zhang, "On the performance of indoor multi-story small-cell networks," *IEEE Trans. Wireless Commun.*, vol. 20, no. 2, pp. 1336–1348, Feb. 2021.
10. Q. Wu and R. Zhang, "Intelligent reflecting surface enhanced wireless network via joint active and passive beamforming," *IEEE Trans. Wireless Commun.*, vol. 18, no. 11, pp. 5394–5409, Nov. 2019.
11. Q. Wu and R. Zhang, "Towards smart and reconfigurable environment: Intelligent reflecting surface aided wireless network," *IEEE Commun. Mag.*, vol. 58, no. 1, pp. 106–112, Jan. 2020.
12. E. Basar, M. Di Renzo, J. D. Rosny, M. Debbah, M.-S. Alouini, and R. Zhang, "Wireless communications through reconfigurable intelligent surfaces," *IEEE Access*, vol. 7, pp. 116753–116773, 2019.
13. T. V. Chien, L. T. Tu, S. Chatzinotas, and B. Ottersten, "Coverage probability and ergodic capacity of intelligent reflecting surfaceenhanced communication systems," *IEEE Commun. Lett.*, vol. 25, no. 1, pp. 69–73, Jan. 2021.
14. T. V. Chien, A. K. Papazafeiropoulos, L. T. Tu, R. Chopra, S. Chatzinotas, and B. Ottersten, "Outage probability analysis of IRSassisted systems under spatially correlated channels," *IEEE Wireless Commun. Lett.*, vol. 10, no. 8, pp. 1815–1819, Aug. 2021.
15. I. Yildirim, A. Uyrus, and E. Basar, "Modeling and analysis of reconfigurable intelligent surfaces for indoor and outdoor applications in future wireless networks," *IEEE Trans. Commun.*, vol. 69, no. 2, pp. 1290–1301, Feb. 2021.
16. J. G. Andrews, F. Baccelli, and R. K. Ganti, "A tractable approach to coverage and rate in cellular networks," *IEEE Trans. Commun.*, vol. 59, no. 11, pp. 3122–3134, Nov. 2011.
17. M. Afshang and H. S. Dhillon, "Fundamentals of modeling finite wireless networks using binomial point process," *IEEE Trans. Wireless Commun.*, vol. 16, no. 5, pp. 3355–3370, May 2017.
18. Q. Wu and R. Zhang, "Beamforming optimization for wireless network aided by intelligent reflecting surface with discrete phase shifts," *IEEE Trans. Commun.*, vol. 68, no. 3, pp. 1838–1851, Mar. 2020.
19. S. Abeywickrama, R. Zhang, Q. Yu, and C. Yuen, "Intelligent reflecting surface: Practical phase shift model and beamforming optimization," *IEEE Trans. Commun.*, vol. 68, no. 9, pp. 5849–5863, Sep. 2020.
20. W. Tang et al., "Wireless communications with reconfigurable intelligent surface: Path loss modeling and experimental measurement," *IEEE Trans. Wireless Commun.*, vol. 20, no. 1, pp. 421–439, Jan. 2021.
21. Y. Zhu, G. Zheng, and K.-K. Wong, "Stochastic geometry analysis of large intelligent surface-assisted millimeter wave networks," *IEEE J. Sel. Areas Commun.*, vol. 38, no. 8, pp. 1749–1762, Aug. 2020.
22. Y. Zhu, L. Wang, K.-K. Wong, and R. W. Heath, Jr., "Secure communications in millimeter wave ad hoc networks," *IEEE Trans. Wireless Commun.*, vol. 16, no. 5, pp. 3205–3217, May 2017.
23. C. Bouras, V. Kokkinos, and A. Papazois, "Financing and pricing small cells in next-generation mobile networks," in *Proc. Wired Wireless Internet Commun.*, Paris, France, May 2014, pp. 41–54.

24. J. Zhang, A. A. Glazunov, and J. Zhang, "Wireless performance evaluation of building layouts: Closed-form computation of figures of merit," *IEEE Trans. Commun.*, vol. 69, no. 7, pp. 4890–4906, Jul. 2021.
25. J. Zhang, A. A. Glazunov, and J. Zhang, "Wireless energy efficiency evaluation for buildings under design based on analysis of interference gain," *IEEE Trans. Veh. Technol.*, vol. 69, no. 6, pp. 6310–6324, Jun. 2020